Synthesis and characterisation of [Fe$_2$M$_3$(μ_4-E)(μ_3-E′)(CO)$_{17}$] and [Os$_3$(μ_3-E)(μ_3-E′)(CO)$_9$] (M = Os or Ru; E = S, Se, Te; E′ = Se, Te)

Pradeep Mathur [a],*, Pramatha Payra [a], Sanjukta Ghose [a], Md. Munkir Hossain [a], C.V.V. Satyanarayana [b], Fernando O. Chicote [c], Raj K. Chadha [c]

[a] *Chemistry Department, Indian Institute of Technology, Powai, Bombay 400 076, India*
[b] *Regional Sophisticated Instrumentation Centre, Indian Institute of Technology, Bombay 400 076, India*
[c] *Centro de Graduados, Instituto Technologica de Tijuana, B.C., Mexico 22000, Mexico*

Dedicated to Professor Heinrich Vahrenkamp on the occasion of his 60th birthday

Abstract

A set of new chalcogen-bridged mixed metal clusters [Fe$_2$Os$_3$(μ_4-E)(μ_3-E′)(CO)$_{17}$] (**2**, EE′ = SeTe; **3**, EE′ = STe; **4**, EE′ = Se$_2$; **5**, EE′ = SSe) and [Fe$_2$Ru$_3$(μ_4-E)(μ_3-E′)(CO)$_{17}$] (**12**, EE′ = SeTe; **13**, EE′ = STe; **14**, EE′ = Se$_2$; **15**, EE′ = SSe) has been synthesised by facile methods. Thermolysis or photolysis of compounds **2**, **3** and **5** afforded the new triosmium mixed chalcogenide clusters [Os$_3$(μ_3-E)(μ_3-E′)(CO)$_9$] (**7**, EE′ = SeTe; **8**, EE′ = STe; **10**, EE′ = SSe). All new compounds were characterised by IR and ^{1}H-, ^{77}Se- and ^{125}Te-NMR spectroscopy. Clusters **8**, **9** and **12** were structurally characterised by single crystal X-ray diffraction methods. © 2000 Published by Elsevier Science S.A. All rights reserved.

Keywords: Iron; Ruthenium; Osmium; Chalcogens; Clusters

1. Introduction

Chemistry of transition metal clusters continues to grow because of their relevance to homogeneous and heterogeneous catalysis [1] and also due to the fact that owing to their low symmetry, they are useful as probes in the study of molecular dynamics of clusters [2]. Bridging single-atom ligands derived from the main groups of the periodic table have been found to play an important role in the synthesis and stabilisation of transition metal cluster compounds [3]. Incorporation of these main group elements into transition metal carbonyl clusters introduces novel structural and reactivity features [4]. Diversity in structural and reactivity features of chalcogen-bridged metal carbonyl complexes has generated interest in the synthesis of new chalcogen bridged complexes and study of their reactions towards inorganic and organic moieties.

Several classes of chalcogen bridged mixed-metal clusters have been synthesised, such as the square pyramidal [Fe$_2$M(μ_3-E)$_2$(CO)$_{10}$] (M = W, E = Se or Te; M = Mo, E = Se) and the octahedral [Fe$_2$Ru$_2$(μ_4-Te)$_2$(CO)$_{11}$] [5]. Different chalcogens exhibit contrasting influence on the reactivity of the chalcogen-bridged species. For instance, whereas [Fe$_2$(μ-Se$_2$)(CO)$_6$] readily adds phenylacetylene at room temperature to yield [Fe$_2$(μ-SeC(Ph)=C(H)Se)(CO)$_6$], the Te-bridged [Fe$_2$(μ-Te$_2$)(CO)$_6$] shows no reactivity under similar conditions; [Fe$_2$(μ-TeC(Ph)=C(H)Te)(CO)$_6$] is formed when a toluene solution containing [Fe$_3$(μ_3-Te)$_2$(CO)$_9$] and phenylacetylene is refluxed [6]. Easy accessibility to the mixed chalcogen compounds [Fe$_3$(μ_3-EE′)(CO)$_9$] and [Fe$_2$(μ-EE′)(CO)$_6$] has now provided an opportunity to investigate the contrasting influence of bridging chalcogen ligands in metal carbonyl complexes. Consequently, several mixed-chalcogen mixed-metal clusters have been prepared. In the square pyramidal cluster series, [Fe$_2$Co(μ_3-E)(μ_3-E′)(CO)$_9$], certain E, E′ combinations have been identified for the cluster to exhibit good NLO properties [7]. Recently we have reported on the

* Corresponding author. Tel.: +91-22-577-4089; fax: +91-22-578-3480.
E-mail address: mathur@ether.chem.iitb.ernet.in (P. Mathur).

synthesis and structure of the tetrahedral cluster series $[Cp_2Mo_2ME(CO)_7]$, (M = Fe, Ru, Os; E = S, Se), and the influence of different E ligands on the NLO properties of these clusters [8].

As part of our investigations of chalcogen-bridged metal carbonyl clusters, we have earlier reported on the synthesis of the tellurium bridged mixed-metal clusters $[Fe_2M_3(\mu_4\text{-}Te)(\mu_3\text{-}Te)(CO)_{17}]$ (M = Ru, Os) [9]. As a continuation of our efforts to develop facile methods for synthesising mixed-metal clusters, we now report on the synthesis and characterisation of a series of clusters of the type $[Fe_2M_3(\mu_4\text{-}E)(\mu_3\text{-}E')(CO)_{17}]$ (E, E′ = S, Se, Te), and on the atom transfer reactions [10] exhibited by them to yield $[M_3(\mu_3\text{-}E)(\mu_3\text{-}E')(CO)_9]$ (M = Os).

2. Results and discussion

2.1. Syntheses

Room temperature reaction of $[Fe_2(\mu\text{-}EE')(CO)_6]$ with $[Os_3(NCMe)(CO)_{11}]$ in benzene yielded the reddish-brown mixed metal cluster compounds, $[Fe_2Os_3(\mu_4\text{-}E)(\mu_3\text{-}E')(CO)_{17}]$ (**1**, EE′ = Te$_2$; **2**, EE′ = SeTe; **3**, EE′ = STe; **4**, EE′ = Se$_2$; **5**, EE′ = SSe) in yields of 35–70% (Scheme 1, Table 1). Also observed in the reaction mixture was a maroon compound, which could not be isolated in pure form and characterised fully due to insufficient amounts. When a benzene solution of

compounds **1**–**5** was irradiated by UV light for 30 min or refluxed for 3 h, the yellow clusters $[Os_3(\mu_3\text{-}E)(\mu_3\text{-}E')(CO)_9]$ (**6**, EE′ = Te$_2$; **7**, EE′ = SeTe; **8**, EE′ = STe; **9**, EE′ = Se$_2$; **10**, EE′ = SSe) were formed in yields of 27–60%. Similarly, room temperature stirring of $[Fe_2(\mu\text{-}EE')(CO)_6]$ (threefold excess) with $[Ru_3(CO)_{12}]$ in benzene solvent yielded the mixed metal clusters $[Fe_2Ru_3(\mu_4\text{-}E)(\mu_3\text{-}E')(CO)_{17}]$ (**11**, EE′ = Te$_2$; **12**, EE′ = SeTe; **13**, EE′ = STe; **14**, EE′ = Se$_2$; **15**, EE′ = SSe) in almost quantitative yields. Table 1 summarises the conditions used for the preparation of **1**–**15** and their spectroscopic data.

Formation of **1**–**5** and **11**–**15** involves a straightforward addition of coordinatively unsaturated 'Os$_3$(CO)$_{11}$' or 'Ru$_3$(CO)$_{11}$' units across the E–E′ bond of $[Fe_2(CO)_6(\mu\text{-}EE')]$, to form the mixed-metal adduct. Overall, there is a formal cleavage of the E–E′ bond and an Os–Os or Ru–Ru bond, and formation of three new chalcogen–osmium or chalcogen–ruthenium bonds respectively. Interestingly there is no new metal–metal bond formation. On UV irradiation, **1**–**5** undergo Fe–chalcogen bond scission and a formal chalcogen transfer occurs from the Fe to Os or Ru metal atoms to form **6**–**10**. Most probably the iron carbonyl fragment decomposes as no iron-containing compound could be isolated after the photolysis.

2.2. Spectroscopic characterisation

The mixed-metal clusters, **1**–**5** and **11**–**15**, and the triosmium clusters **6**–**10** were characterised by IR and ^{77}Se- and ^{125}Te-NMR spectroscopy (Table 1). The IR spectra of **2**–**5** and **12**–**15** display an identical CO stretching pattern, similar to the one reported for **1** and **11** [9] and the spectra of the osmium clusters **6**–**10** display a CO stretching pattern typical for compounds of the form $[M_3(CO)_9(\mu_3\text{-}E)_2]$ [9b]. In both sets of compounds, there is a regular decrease in the stretching frequencies of corresponding bands along the E, E′ combination: SSe > SeSe > STe > TeTe. Previous work has demonstrated the usefulness of ^{77}Se- and ^{125}Te-NMR spectroscopy to differentiate between triply and quadruply bridging modes of these chalcogen atoms; the signals for former appear upfield of the signals for latter. Thus, in the mixed-chalcogen compounds, **2**, **3**, **5**, **12**, **13** and **15**, it has been possible to identify the bonding modes of the two different chalcogen atoms. The lighter chalcogen preferentially bonds in a quadruply bridging mode while the heavier one triply bridges.

2.3. Molecular structures of compounds 8 and 9

The structures of the compounds **8** and **9** have been elucidated by single crystal X-ray diffraction methods. Crystal data and relevant structural parameters are enumerated in Table 2. A representative molecular

Os	Ru	E	E′
1	11	Te	Te
2	12	Se	Te
3	13	S	Te
4	14	Se	Se
5	15	S	Se

Os	E	E′
6	Te	Te
7	Te	Se
8	S	Te
9	Se	Se
10	S	Se
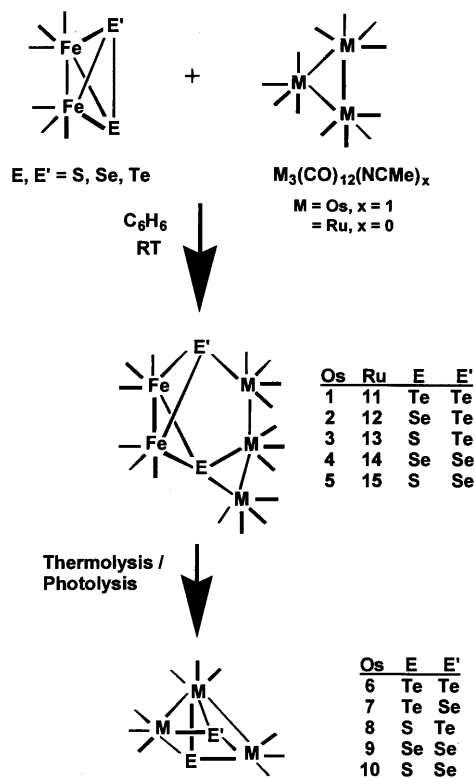
Scheme 1.

Table 1
Preparation of $[M_3Fe_2(\mu_4\text{-}E)(\mu_3\text{-}E')(CO)_{17}]$ (M = Os, Ru; E, E' = S, Se or Te) and $[Os_3(\mu_3\text{-}E)(\mu_3\text{-}E')(CO)_9]$ (E, E' = S, Se or Te)

Product	Reactants (mg; mmol)	Yield (mg (%))	IR (ν(CO) cm^{-1}, hexane)	Carbon analysis (% (found))	^{77}Se-NMR (δ, CDCl$_3$)	^{125}Te-NMR (δ, CDCl$_3$)
$[Os_3Fe_2(\mu_4\text{-}Te)(\mu_3\text{-}Te)(CO)_{17}]$ (1)	$[Fe_2(\mu\text{-}Te_2)(CO)_6]$ (246; 0.46) + $[Os_3(CO)_{11}(NCMe)]$ (180; 0.20)	196 (70)	2127(w), 2099(m), 2069(w), 2057(m), 2053(vs), 2044(m), 2039(m), 2022(m), 2015(w), 1996(m), 1989(w), 1973(m), 1965(w)	14.44 (14.31)		+70, −251
$[Os_3Fe_2(\mu_4\text{-}Se)(\mu_3\text{-}Te)(CO)_{17}]$ (2)	$[Fe_2(\mu\text{-}SeTe)(CO)_6]$ (96; 0.22) + $[Os_3(CO)_{11}(NCMe)]$ (90; 0.14)	80 (60)	2129(w), 2101(s), 2058(m, sh), 2054(vs), 2044(s), 2040(w,sh), 2023(w), 2016(w), 1996(m), 1987(w), 1972(m), 1965(w)	14.96 (14.83)	−76	−224
$[Os_3Fe_2(\mu_4\text{-}S)(\mu_3\text{-}Te)(CO)_{17}]$ (3)	$[Fe_2(\mu\text{-}STe)(CO)_6]$ (220; 0.53) + $[Os_3(CO)_{11}(NCMe)]$ (225; 0.25)	163 (50)	2130(w), 2090(m), 2064(w, sh), 2061(w, sh), 2056(vs), 2036(w, sh), 2025(s), 2010(w), 2000(s), 1992(m), 1978(m)	15.49 (15.25)		−177
$[Os_3Fe_2(\mu_4\text{-}Se)(\mu_3\text{-}Se)(CO)_{17}]$ (4)	$[Fe_2(\mu\text{-}Se_2)(CO)_6]$ (44; 0.13) + $[Os_3(CO)_{11}(NCMe)]$ (50; 0.05)	36 (50)	2131(w), 2104(s), 2076(m), 2063(m,sh), 2056(vs), 2043(s), 2041(w, sh), 2025(w), 2015(w), 2000(m), 1989(w), 1972(w), 1964(w)	15.51 (15.38)	−75, −143	
$[Os_3Fe_2(\mu_4\text{-}S)(\mu_3\text{-}Se)(CO)_{17}]$ (5)	$[Fe_2(\mu\text{-}SSe)(CO)_6]$ (78; 0.23) + $[Os_3(CO)_{11}(NCMe)]$ (90; 0.12)	43 (35)	2132(m), 2118(s), 2105(s), 2092(m), 2077 (s), 2067(w), 2057(vs), 2044(s), 2032(w), 2029(w), 2024(w, sh), 2017(w), 2011(w), 1995(s), 1982(w), 1979(s), 1963(m)	16.08 (15.92)	−98	
$[Os_3(\mu_3\text{-}Te)_2(CO)_9]$ (6)	1 (100; 0.07)	46 (60)	2069(s), 2049(s), 2010(s)	10.03 (9.82)		−355
$[Os_3(\mu_3\text{-}Se)(\mu_3\text{-}Te)(CO)_9]$ (7)	2 (50; 0.04)	21 (55)	2073(s), 2053(s), 2013(s)	10.50 (10.33)	−115	−371
$[Os_3(\mu_3\text{-}Se)_2(CO)_9]$ (9)	4 (30; 0.02)	10 (45)	2076(s), 2056(s), 2015(s)	11.02 (10.79)	−120	
$[Os_3(\mu_3\text{-}S)(\mu_3\text{-}Se)(CO)_9]$ (10)	5 (35; 0.03)	7 (27)	2078(s), 2058(s), 2017(s)	11.58 (11.37)	−201	
$[Ru_3Fe_2(\mu_4\text{-}Te)(\mu_3\text{-}Te)(CO)_{17}]$ (11)	$[Fe_2(\mu\text{-}Te_2)(CO)_6]$ (123; 0.23) + $[Ru_3(CO)_{12}]$ (45; 0.07)	59 (73)	2122(w), 2093(m), 2053(vs), 2039(m), 2028(w), 2020(m), 1994(m), 1985(w)	17.81 (17.66)		−407, +394
$[Ru_3Fe_2(\mu_4\text{-}Se)(\mu_3\text{-}Te)(CO)_{17}]$ (12)	$[Fe_2(\mu\text{-}SeTe)(CO)_6]$ (49; 0.12) + $[Ru_3(CO)_{12}]$ (22; 0.03)	27 (72)	2124(w), 2094(s), 2055(vs), 2050(s, sh), 2041(m, sh), 2021(m), 1994(s), 1984(m)	18.61 (18.45)	−175	−237
$[Ru_3Fe_2(\mu_4\text{-}S)(\mu_3\text{-}Te)(CO)_{17}]$ (13)	$[Fe_2(\mu\text{-}STe)(CO)_6]$ (101; 0.23) + $[Ru_3(CO)_{12}]$ (50; 0.08)	57 (70)	2126(w), 2095(m), 2056(vs), 2049(s, sh), 2042(m, sh), 2021(w), 1993(w), 1981(w)	19.44 (19.27)		−229
$[Ru_3Fe_2(\mu_4\text{-}Se)(\mu_3\text{-}Se)(CO)_{17}]$ (14)	$[Fe_2(\mu\text{-}Se_2)(CO)_6]$ (66; 0.15) + $[Ru_3(CO)_{12}]$ (32; 0.05)	18 (36)	2126(m), 2098(m), 2062(s), 2057(vs), 2049(s, sh), 2024(m), 1996(m), 1985(m)	19.47 (19.31)	+172, −148	
$[Ru_3Fe_2(\mu_4\text{-}S)(\mu_3\text{-}Se)(CO)_{17}]$ (15)	$[Fe_2(\mu\text{-}SSe)(CO)_6]$ (90; 0.23) + $[Ru_3(CO)_{12}]$ (50; 0.08)	10 (17)	2127(w), 2099(s), 2063(s, sh), 2057(vs), 2049(s, sh), 2025(w), 1999(s), 1986(m, br), 1983(m, br)	20.38 (20.14)	−142	

Table 2
Crystal data and structure refinement for [Os$_3$(μ_3-E)(μ_3-E')(CO)$_9$] (STe, **8**; Se$_2$, **9**) and [Ru$_3$Fe$_2$(μ_4-Se)(μ_3-Te)(CO)$_{17}$] (**12**)

	8	**9**	**12**
Empirical formula	C$_9$O$_9$Os$_3$STe	C$_9$O$_9$Os$_3$Se$_2$	C$_{17}$O$_{17}$Fe$_2$Ru$_3$SeTe
Formula weight	982.35	979.4	1097.64
$F(000)$	1688	808	2032
Crystal system, space group	Monoclinic, $P2_1/C$	Triclinic, $P\bar{1}$	Orthorhombic, $Pnn2$
Unit cell dimensions			
a (Å)	6.682(1)	6.7706(8)	16.0867(1)
b (Å)	17.983(7)	9.5603(13)	18.131(2)
c (Å)	13.689(3)	13.534(2)	9.9533(9)
α (°)	90	82.211(9)	90
β (°)	96.16(3)	84.555 (9)	90
γ (°)	90	69.372(11)	90
V (Å^3)	1635(1)	811.3(2)	2903.0(4)
Z	4	2	4
D_{calc} (Mg m^{-3})	3.990	3.822	2.511
Crystal size (mm^3)	$0.38 \times 0.26 \times 0.22$	$0.22 \times 0.19 \times 0.16$	$0.50 \times 0.42 \times 0.28$
Temperature (K)	296(2)	296(2)	296(2)
Scan type	2θ–θ	2θ–θ	2θ–θ
Data collection range θ (°)	2.27 to 22.54	2.29 to 24.99	2.25 to 24.99
Index ranges	$0 \leq h \leq 7$, $0 \leq k \leq 19$, $-14 \leq l \leq 14$	$-1 \leq h \leq 7$, $-10 \leq k \leq 11$, $-16 \leq l \leq 16$	$-1 \leq h \leq 19$, $-1 \leq k \leq 21$, $-1 \leq l \leq 11$
Reflections collected/unique	2458/2148 [$R_{int} = 0.0000$]	3606/2825 [$R_{int} = 0.0561$]	3482/3035 [$R_{int} = 0.0243$]
Data/restraints/parameters	2142/0/179	2825/0/209	3035/0/370
Goodness of fit on F^2 (s)	1.024	1.076	1.036
Final R indices [$I > 2\sigma(I)$] [a]	$R_1 = 0.0421$, $wR_2 = 0.1049$	$R_1 = 0.0545$, $wR_2 = 0.1551$	$R_1 = 0.0252$, $wR_2 = 0.0588$
Final R indices (all data)	$R_1 = 0.0759$, $wR_2 = 0.1208$	$R_1 = 0.0606$, $wR_2 = 0.1617$	$R_1 = 0.0303$, $wR_2 = 0.0615$
Goodness of fit	1.024	1.076	1.036
Largest difference peak and hole (e Å^{-3})	2.293 and -1.859	2.907 and -4.064	0.504 and -0.427

[a] $R_1 = (\Sigma|||F_o|| - ||F_c|||/\Sigma||F_o||)$, $wR_2 = \Sigma w(F_o^2 - F_c^2)^2/\Sigma w[(F_o^2)^2]^{1/2}$, $s = [\Sigma w(F_o^2 - F_c^2)^2/(n-p)]^{1/2}$.

structure of [Os$_3$(μ_3-E)(μ_3-E')(CO)$_9$] (**8**, EE' = STe, and **9**, EE' = Se$_2$) is depicted in Fig. 1. Selected bond lengths and bond angles for **8** and **9** are listed in Tables 3 and 4 respectively. All three clusters have an identical heavy atom skeleton consisting of an Os$_3$EE' square pyramid in which the apical site is occupied by one of the Os atoms. Each Os atom has three terminal CO groups. The average Os–Os bond lengths in **8** (2.841 Å) and **9** (2.821 Å) are similar to that reported for [Os$_3$(CO)$_{12}$] (2.877(1) Å) [11], but shorter than the > 2.92 Å Os–Os bond lengths in the cluster [Os$_4$(μ_3-Se)$_2$(CO)$_{12}$] [12]. The average Os–Se bond length in **9** (2.487 Å) is slightly shorter than the average Os–Se bond lengths (2.53 and 2.556 Å) in [Os$_4$(μ_3-Se)$_2$(CO)$_{12}$] and [H$_2$Os$_4$(μ_3-Se)$_2$(CO)$_{12}$] respectively [12]. The average Os–S bond length of **8** (2.439 Å) is comparable to that in [Os$_4$(μ_3-S)$_2$(CO)$_{12}$] (2.411 Å) and within the range of Os–S bond distances found typically for triply bridging sulfido ligands observed in osmium clusters [13].

In compounds **6–10** the chalcogen ligands adopt the μ_3-bridging mode and hence function as four electron donors to the cluster. In terms of electron counting rules, these are 50-electron clusters, and the formal application of the 18-electron rule would predict two metal–metal bonds as is observed.

2.4. Molecular structure of compound **12**

The molecular structure of [Fe$_2$Ru$_3$(μ_4-Se)(μ_3-Te)(CO)$_{17}$] (**12**) is shown in Fig. 2. Crystal data and structure refinement are listed in Table 2. Selected bond lengths and bond angles of **12** are given in Table 5. The structure is similar to the previously reported [Fe$_2$Ru$_3$(μ_4-Te)(μ_3-Te)(CO)$_{17}$] (**11**) [9a]. The metal core geometry can be best described as an Fe$_2$SeTe butterfly arrangement, with the two wing-tip chalcogens bridged by a bent 'Ru$_3$(CO)$_{11}$' unit. The lighter chalcogen adopts a quadruply bridging mode, whereas the heavier Te atom is triply bridged. The average Ru–Ru bond distance (2.910 Å) and Fe(1)–Fe(2) bond distance (2.605(2) Å) in **12** are slightly shorter than those in **11** (2.950 and 2.650(2) Å respectively). On the other hand, the average Fe–Te bond length (2.591 Å) and Ru(3)–Te bond length (2.7957(9) Å) in **12** are slightly longer than the corresponding bond lengths in **11** (2.5405 and 2.6215(1) Å respectively). The Fe–Se (2.3348 Å) and Ru–Se (2.4639 Å) bonds are shorter than those in [Fe$_3$Ru(μ_4-Se)$_2$(CO)$_{11}$] [14] (2.495(1) and 2.5545(1) Å respectively).

The compounds [Fe$_2$M$_3$((μ_4-E)((μ_3-E')(CO)$_{17}$] are 84-electron clusters. Assuming that the μ_4-E is a six-elec-
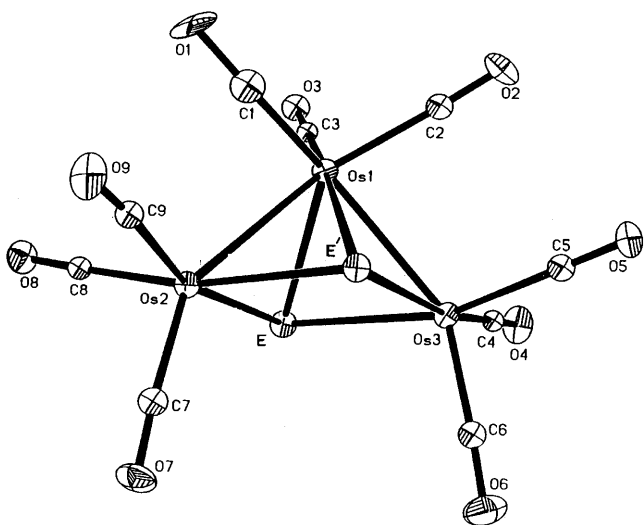
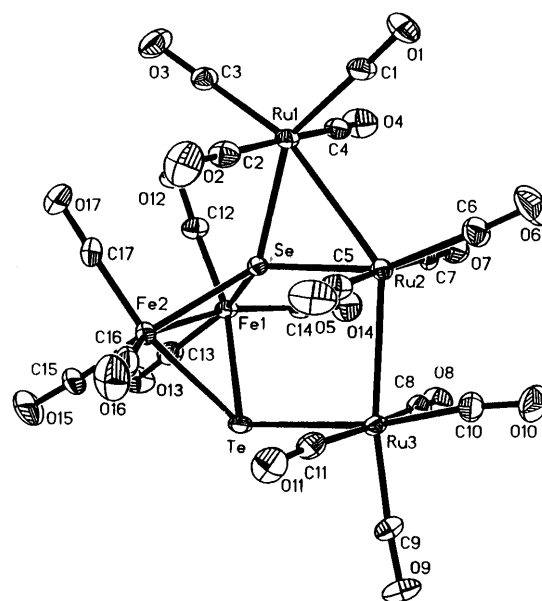Fig. 1. Representative molecular structure of $[Os_3(\mu_3\text{-}E)(\mu_3\text{-}E')(CO)_9]$ (**8**, EE′ = STe and **9**, EE′ = SeSe).

Fig. 2. Molecular structure of $[Ru_3Fe_2(\mu_4\text{-}Se)(\mu_3\text{-}Te)(CO)_{17}]$ (**12**).

Table 3
Selected bond lengths (Å) and angles (°) for compound **8**

Os(1)–Te(1)	2.723(2)	Os(2)–S(1)	2.428(5)
Os(3)–Te(1)	2.648(2)	Os(1)–S(1)	2.462(5)
Os(2)–Te(1)	2.652(2)	Os(3)–S(1)	2.426(5)
Os(1)–Os(2)	2.8416(13)	Os(1)–Os(3)	2.840(2)
Te(1)–Os(1)–Os(3)	56.81(4)	S(1)–Os(1)–Te(1)	78.87(13)
Te(1)–Os(3)–Os(1)	59.38(5)	S(1)–Os(1)–Os(3)	53.89(12)
S(1)–Os(1)–Os(2)	53.92(12)	Te(1)–Os(1)–Os(2)	56.87(4)
S(1)–Os(2)–Os(1)	55.03(12)	Te(1)–Os(2)–Os(1)	59.32(5)
S(1)–Os(2)–Te(1)	80.90(14)	S(1)–Os(3)–Te(1)	81.01(13)
Os(3)–Os(1)–Os(2)	85.17(4)	S(1)–Os(3)–Os(1)	55.08(12)
Os(3)–Te(1)–Os(1)	63.81(5)	Os(3)–Te(1)–Os(2)	92.99(6)
Os(3)–S(1)–Os(2)	104.8(2)	Os(2)–Te(1)–Os(1)	63.81(5)
Os(2)–S(1)–Os(1)	71.1(2)	Os(3)–S(1)–Os(1)	71.0(2)

Table 5
Selected bond lengths (Å) and angles (°) for **12**

Ru(1)–Se	2.4861(9)	Ru(2)–Se	2.4417(10)
Ru(2)–Ru(3)	2.9238(9)	Ru(1)–Ru(2)	2.8964(10)
Te–Fe(1)	2.5894(12)	Te–Ru(3)	2.7957(9)
Se–Fe(2)	2.334(2)	Te–Fe(2)	2.592(2)
Se–Fe(1)	2.3356(13)	Fe(1)–Fe(2)	2.605(2)
Se–Ru(1)–Ru(2)	53.29(2)	Ru(1)–Ru(2)–Ru(3)	140.32(3)
Se–Ru(2)–Ru(1)	54.72(3)	Ru(1)–Se–Ru(2)	71.99(3)
Se–Ru(2)–Ru(3)	85.68(3)	Te–Ru(3)–Ru(2)	98.41(3)
Fe(1)–Te–Ru(3)	109.57(3)	Fe(2)–Te–Ru(3)	109.57(4)
Fe(2)–Se–Fe(1)	67.82(5)	Fe(1)–Te–Fe(2)	60.37(4)
Fe(1)–Se–Ru(2)	130.93(5)	Fe(2)–Se–Ru(2)	134.26(5)
Fe(1)–Se–Ru(1)	132.00(4)	Fe(2)–Se–Ru(1)	131.53(5)
Te–Fe(1)–Fe(2)	59.86(4)	Te–Fe(2)–Fe(1)	59.77(4)
Se–Fe(2)–Te	79.86(5)	Se–Fe(1)–Te	79.88(4)
Se–Fe(2)–Fe(1)	56.12(4)	Se–Fe(1)–Fe(2)	56.06(4)

Table 4
Selected bond lengths (Å) and angles (°) for compound **9**

Os(1)–Se(4)	2.483(3)	Os(1)–Se(5)	2.462(3)
Os(2)–Se(4)	2.478(3)	Os(2)–Se(5)	2.458(3)
Os(3)–Se(4)	2.529(3)	Os(3)–Se(5)	2.514(3)
Os(1)–Os(3)	2.8252(11)	Os(2)–Os(3)	2.8179(11)
Se(4)–Os(1)–Os(3)	56.45(6)	Se(5)–Os(1)–Se(4)	81.61(9)
Se(5)–Os(2)–Os(4)	81.80(10)	Se(5)–Os(1)–Os(3)	56.29(7)
Se(5)–Os(2)–Os(3)	56.43(7)	Se(4)–Os(2)–Os(3)	56.60(6)
Se(4)–Os(3)–Os(2)	54.90(6)	Se(5)–Os(3)–Se(4)	79.71(10)
Se(5)–Os(3)–Os(1)	54.53(7)	Se(5)–Os(3)–Os(2)	54.53(7)
Os(2)–Os(3)–Os(1)	82.42(3)	Se(4)–Os(3)–Os(1)	54.93(6)
Os(2)–Se(4)–Os(3)	68.50(7)	Os(2)–Se(4)–Os(1)	97.07(10)
Os(2)–Se(5)–Os(1)	98.19(11)	Os(1)–Se(4)–Os(3)	68.62(7)
Os(1)–Se(5)–Os(3)	69.18(8)	Os(2)–Se(5)–Os(3)	69.04(8)

tron donor ligand and the $\mu_3\text{-}E'$ is a four-electron donor ligand, application of the 18-electron rule predicts the presence of three metal–metal bonds, as observed. The set of compounds **1–5** and **11–15** represent unique examples of clusters where the wing tip chalcogen atoms are bridged by polynuclear coordinatively unsaturated metal fragments.

3. Experimental

3.1. General procedures

All reactions and other manipulations were carried out using standard Schlenk techniques under an inert atmosphere of argon. All solvents were purified, dried

and distilled under a nitrogen or argon atmosphere immediately prior to use. Reactions were monitored by TLC as well as by FTIR spectroscopy. Infrared spectra were recorded on a Nicolet Impact 400 FTIR spectrophotometer as hexane solutions in 0.1 mm path length NaCl cells. Elemental analyses were performed using a Carlo Erba automatic analyser. ^{77}Se- and [125]Te-NMR spectra were recorded on a Varian VXR-300S spectrometer in $CDCl_3$. Operating frequency for ^{77}Se-NMR was 57.23 MHz; 90° pulses were used with 1.0 s delay and 1.0 s acquisition time. Operating frequency for [125]Te was 94.705 MHz with pulse of 90° and a delay of 1.0 s. ^{77}Se-NMR spectra are referenced to Me_2Se ($\delta = 0$) and [125]Te-NMR spectra are referenced to Me_2Te ($\delta = 0$). The starting materials $[Fe_2(\mu-E_2)(CO)_6]$ (E = S, Se, Te) [15], $[Fe_2(\mu-STe)(CO)_6]$ [16], $[Fe_2(\mu-SeTe)(CO)_6]$ [17], $[Fe_2(\mu-SSe)(CO)_6]$ [18] and $[M_3(CO)_{12-x}(NCMe)_x]$ (M = Ru, Os; x = 1, 2) [19] were prepared by established procedures. $[Ru_3(CO)_{12}]$ and $[Os_3(CO)_{12}]$ were purchased from Strem Chemicals (USA) and used as such. Photochemical reactions were carried out in a water-cooled double-walled quartz vessel having a 125 W immersion-type mercury lamp manufactured by Applied Photophysics Ltd. Quantities of reactants used and yields of products obtained are given in Table 1.

3.2. Preparation of [Os₃Fe₂(μ₄-E)(μ₃-E′)(CO)₁₇] and [Os₃(μ₃-E)(μ₃-E′)(CO)₉] (E = S, Se, Te; E′ = Se, Te)

In a typical preparation twofold excess of $[Fe_2(\mu-EE')(CO)_6]$ (E = S, Se, Te; E′ = Se, Te) in benzene was stirred with a benzene solution of $[Os_3(NCMe)(CO)_{11}]$ at room temperature for 5 h. The solvent was removed in vacuum, and the residue subjected to chromatographic work-up on a silica gel column. Using hexane–dichloromethane (80:20, v/v) mixture as eluent, the following bands were obtained, in order of elution: brown $[Fe_3(\mu_3-E)(\mu_3-E')(CO)_9]$ together with yellow $[Os_3(CO)_{12}]$ (trace), unreacted $[Fe_2(\mu-EE')(CO)_6]$, reddish orange $[Os_3Fe_2(\mu_4-E)(\mu_3-E')(CO)_{17}]$ (1, E = E′ = Te; 2, E = Se, E′ = Te; 3, E = S, E′ = Te; 4, E = E′ = Se; 5, E = S, E′ = Se) and a maroon compound.

When a benzene solution (50 ml) of **1–5** was irradiated by UV light under a constant purge of argon for 30 min or was subjected to thermolytic conditions for 3 h, the colour of the solution changed from orange to light yellow. The reaction mixture was filtered and after removal of the solvent in vacuo, the residue was subjected to chromatographic work-up using a silica gel column. Using hexane as eluent, yellow $[Os_3(\mu_3-E)(\mu_3-E')(CO)_9]$ (6, E = E′ = Te; 7, E = Se, E′ = Te; 8, E = S, E′ = Te; 9, E = E′ = Se; 10, E = S, E′ = Se) was obtained. These compounds **6–10** could also be syn-

thesised from a room temperature reaction of $[Os_3(NCMe)_2(CO)_{10}]$ and $[Fe_2(\mu-EE')(CO)_6]$.

3.3. Preparation of [Ru₃Fe₂(μ₄-E)(μ₃-E′)(CO)₁₇] (E = S, Se, Te; E′ = Se, Te)

A benzene solution (50 ml) of $[Fe_2(\mu-EE')(CO)_6]$ (twofold excess) was stirred with $[Ru_3(CO)_{12}]$ at room temperature for 8 h. The solvent was removed under vacuum and the residue was dissolved in 100 ml CH_2Cl_2. This solution was filtered through a Celite pad and chromatographed on a silica gel column. Elution with hexane afforded $[Ru_3(\mu_3-E)(\mu_3-E')(CO)_9]$ (trace), $[Fe_2Ru(\mu_3-E)(\mu_3-E')(CO)_9]$, unreacted $[Ru_3(CO)_{12}]$ and $[Fe_2(\mu-EE')(CO)_6]$. Further elution with a hexane–dichloromethane (90:10, v/v) solvent mixture gave the maroon compounds $[Ru_3Fe_2(\mu_4-E)(\mu_3-E')(CO)_{17}]$ (11, E = E′ = Te; 12, E = Se, E′ = Te; 13, E = S, E′ = Te; 14, E = E′ = Se; 15, E = S, E′ = Se).

3.4. Crystal structure determination of compounds 8, 9 and 12

Orange plate like crystals of **8** and brown, parallelopiped crystals of **9** and **12** suitable for X-ray diffraction analysis were grown from *n*-hexane and dichloromethane solvent mixtures by slow evaporation of the solvents at −5°C. The data were collected on a Siemens P4 diffractometer for compounds **9** and **12** and on a Rigaku AFC6S diffractometer for **8**, using graphite monochromated Mo–K_α radiation ($\lambda = 0.71073$ Å). Unit cell dimensions and standard deviations were obtained by least squares fit to 25 reflections ($15 < 2\theta < 30°$). The data were corrected for Lorentz and polarisation effects and an absorption correction based on a psi-scan was also applied. The structures for **9** and **12** were solved by direct methods using the program SHELXTL version 5, whereas in the case of **8**, SHELXS 86 was used [20]. For compound **8**, osmium, chalcogens, oxygen and C1–C3 atoms were refined anisotropically while C4–C9 atoms were refined isotropically by the full matrix least-squares method. For **9** and **12**, all non-hydrogen atoms were refined anisotropically by the full matrix least-squares method. The function minimised was $\Sigma w(\|F_o\| - \|F_c\|^2)$. A weighting scheme of the form $w = 1/[\sigma^2(F_o)^2 + (aP)^2 + bP]$ (with $a = 0.0612$ and $b = 27.58$ for **8**, $a = 0.0926$ and $b = 34.55$ for **9**, and $a = 0.0326$ and $b = 0.0$. for **12**; P, defined as $\max(F_o^2, 0) + 2F_c^2)/3$) was used. An extinction correction was also applied to the data. The refinement converged to the R indices given in Table 2, which also includes the largest difference peak and hole in the last cycles of refinement.

The structures for **9** and **12** were solved on a Silicon graphics INDY and an IBM compatible PC using the programs X-scans (data reduction) and SHELXTL-PC (refinement and plotting) [21]. The structure for **8** was solved on a Silicon Graphics Personal Iris 4D/35 and an IBM compatible PC using programs TEXSAN (data reduction) [22], SHELXL-93 (refinement) [23] and SHELXTL-PC (plotting).

4. Supplementary material

Crystallographic data for the structural analysis have been deposited with the Cambridge Crystallographic Data Centre, CCDC nos. 142046–142049. Copies of the information may be obtained free of charge from The Director, CCDC, 12 Union Road, Cambridge CB2 1EZ, UK (fax: + 44-1223-336063; e-mail: deposit@ccdc.cam.ac.uk or www: http://www.ccdc.cam.ac.uk).

References

[1] (a) P. Braunstein, L.A. Oro, P.R. Raithby (Eds), Metal Clusters in Chemistry, Wiley-VCH, Weinheim, 1999. (b) G. Süss-Fink, G. Meister, Adv. Organomet. Chem. 35 (1993) 41. (c) S. Bhaduri, P. Mathur, P. Payra, K. Sharma, J. Am. Chem. Soc. 120 (1998) 12127.

[2] (a) W.L. Gladfelter, G.L. Geoffroy, Adv. Organomet. Chem. 18 (1980) 207. (b) K.H. Whitmire, J. Coord. Chem. 17 (1988) 95.

[3] (a) M.A. Ansari, J.A. Ibers, Coord. Chem. Rev. 100 (1990) 223. (b) L.C. Roof, J.W. Kolis, Chem. Rev. 93 (1993) 1037. (c) L.N. Lewis, Chem. Rev. 93 (1993), 2693.

[4] (a) P. Mathur, Adv. Organomet. Chem. 41 (1997) 243. (b) P. Mathur, D. Chakrabarty, M.M. Hossain, R.S. Rashid, V. Rugmini, A.L. Rheingold, Inorg. Chem. 31 (1992) 1106. (c) P. Mathur, M.O. Ahmed, A.K. Dash, M.G. Walawalkar, J. Chem. Soc. Dalton Trans. (1999) 1795.

[5] (a) P. Mathur, P. Sekar, C.V.V. Satyanarayana, M.F. Mahon, J. Chem. Soc. Dalton Trans. (1996) 2173. (b) P. Mathur, I.J. Mavunkal, V. Rugmini, M.F. Mahon, Inorg. Chem. 29 (1990) 4838.

[6] (a) T. Fassler, D. Buchholz, G. Huttner, J. Zsolnai, J. Organomet. Chem. 369 (1989) 297. (b) P. Mathur, M.M. Hossain, Organometallics 12 (1993) 2398.

[7] S. Banerjee, G.R. Kumar, P. Mathur, P. Sekar, Chem. Commun. (1997) 299.

[8] P. Mathur, S. Ghose, M.M. Hossain, C.V.V. Satyanarayana, R.K. Chadha, S. Banerjee, G.R. Kumar, J. Organomet. Chem. 568 (1998) 197.

[9] (a) P. Mathur, I.J. Mavunkal, A.L. Rheingold, J. Chem. Soc., Chem. Commun. (1982) 253. (b) P. Mathur, I.J. Mavunkal, V. Rugmini, Inorg. Chem. 28 (1989) 3616.

[10] (a) S. Nakanishi, M. Yasui, N. Kihara, T. Takata, Chem. Lett. (1999) 843. (b) X.L. Cui, Y.J. Wu, C.X. Du, L.R. Yang, Y. Zhu, Tetrahedron: Asymmetry 10 (1999) 1255.

[11] M.R. Churchill, B.G. Deboer, Inorg. Chem. 16 (1977) 878.

[12] (a) R.D. Adams, I.T. Horvath, Inorg. Chem. 23 (1984) 4718. (b) B.F.G. Johnson, J. Lewis, P.G. Lodge, P.R. Raithby, K. Henrick, M. McPartlin, J. Chem. Soc. Chem. Commun. (1979) 719.

[13] (a) R.D. Adams, I.T. Horvath, P. Mathur, B.E. Segmuller, L.W. Yang, Organometallics 2 (1983) 1078. (b) R.D. Adams, L.W. Yang, J. Am. Chem. Soc. 105 (1983) 235.

[14] P. Mathur, M.M. Hossain, R.S. Rashid, J. Organomet. Chem. 467 (1994) 245.

[15] W. Heiber, J.Z. Gruber, Anorg. Allg. Chem. 91 (1958) 298.

[16] P. Mathur, D. Chakrabarty, M.M. Hossain, R.S. Rashid, J. Organomet. Chem. 420 (1991) 79.

[17] D. Chakrabarty, M.M. Hossain, R.K. Kumar, P. Mathur, J. Organomet. Chem. 410 (1991) 143.

[18] P. Mathur, P. Sekar, C.V.V. Satyanarayana, M.F. Mahon, Organometallics 12 (1993) 1988.

[19] (a) B.F.G. Johnson, J. Lewis, D.A. Pippard, J. Chem. Soc. Dalton Trans. (1981) 407. (b) P.A. Dawson, B.F.G. Johnson, J. Lewis, J. Puga, P.R. Raithby, M.J. Rosales, J. Chem. Soc. Dalton Trans. (1982) 253.

[20] G.M. Sheldrick, Acta Crystallogr. Sect. A 46 (1990) 467.

[21] G.M. Sheldrick, SHELXTL-PC, Siemens Analytical X-ray Instruments Inc., Madison, WI, 1990.

[22] TEXSAN, Structure Analysis Package, Molecular Structure Corporation, The Woodlands,TX, 1992.

[23] G.M. Sheldrick, SHELXL-93, A computer program for crystal structure refinement, University of Göttingen, 1993.